International Journal of Bioelectromagnetism
Vol. 13, No. 4, pp. 190-194, 2011

Assessing Catheter Contact in Radiofrequency Cardiac Ablation Using Complex Impedance

Neal P. Gallagher[a], Israel J. Byrd[b], Elise C. Fear[a], Edward J. Vigmond[a]

[a]Dept. Electrical and Computer Engineering, University of Calgary, Calgary, Alberta, CANADA
[b]St. Jude Medical, Minneapolis, Minnesota, UNITED STATES
Correspondence: N.P.Gallagher, Electrical and Computer Engineering, University of Calgary, Calgary, CANADA, T2N 1N4
E-mail: nealgall@telus.net, phone +1 403 220 8798, fax +1 403 282 6855

Abstract. One of the most important factors in a successful ablation procedure is catheter-endocardial contact. There is little information available to predict the geometric factors that affect this (depth or angle). We present a method that uses a computer model to calculate the complex electrical impedance between an ablation catheter and dispersive electrode. This method takes into account a more realistic ablation scenario that also considers not just penetration depth but also several different catheter angles. We predict that the impedance is a better indicator of catheter-endocardial contact area then just simply penetration depth. It is found that there is an extremely high correlation between increasing impedance and catheter-endocardial tissue contact area. This is clinically relevant because it allows the operating physician to know how well engaged the catheter is with the tissue given the measured complex impedance.

Keywords: RF Ablation, Complex Impedance, Atrial Fibrillation, Rhythm Control, Cardiovascular system

1. Introduction

Radio-Frequency (RF) catheter ablation is a proven method in the treatment of cardiac arrhythmia such as supraventricular tachycardia and particularly atrial fibrillation (AF) [Wittkampf and Nakagawa, 2006]. In the procedure, the physician advances the catheter to the target site in the heart, generally around the pulmonary veins [Ho et al., 1999] (for AF), through a venous access point. From there, the catheter tip is positioned at the target endocardial site with the aid of fluoroscopy. Once in place, an RF current is applied which flows between the catheter and a dispersive patch electrode placed on the surface of the patient's body. This current heats the myocardial tissue via the Joule effect and at temperatures in excess of 50°C, cellular necrosis sets in (caused by protein denaturation of the cellular membrane) which results in a permanent loss of electrical excitability [Nath et al., 1993]; ideally eliminating or confining the arrhythmic focus.

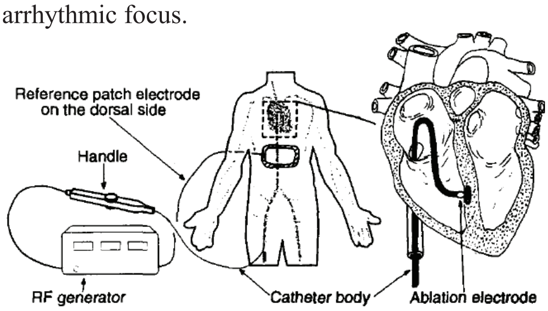

Figure 1. *Schematic of RF cardiac catheter ablation. Figure depicts a ventricular ablation but a similar approach would be taken for an atrial ablation.*

The success of this procedure is entirely dependent on proper transmural lesion formation [Panescu et al., 1995]. Of all the factors that influence lesion formation, local catheter-endocardial contact geometry (penetration depth and incident angle) is the one that is least well controlled due to a lack of soft tissue contrast in the fluoroscopy images. There are significant safety concerns associated with this uncertainty: should the catheter remain in the blood pool instead of engaged with the myocardium thrombi [Gaita et al., 2010] and steam can be produced (both which are potentially lethal), as well as pulmonary vein stenosis and damage to the esophagus.

Clearly, work must be done to characterize the catheter contact. One of the most elegant ways of doing this is by using the measured electrical impedance as this is potentially a powerful indicator of the electrical coupling between the catheter and the tissue. Attempts have been made to characterize the penetration depth using fitted splines and impedance ratio/differencing [Cao et al., 2002], yet they only take into account the impedance magnitude and consider only scenarios where the catheter is incident at 90° with the tissue. This is not representative of an actual ablation scenario as the catheter can be incident upon the tissue at any number of angles. This work seeks to assess catheter contact using complex impedance (both resistance and reactance) given a full set of catheter-tissue penetration depths and incident contact angles. Unfortunately, direct measurement of electric fields is challenging from an in-situ standpoint, but the dynamics of the system can be carefully studied using an advanced computer model. If the complex impedance of the system can be accurately calculated in a model, then it should be possible to non-invasively correlate the complex impedance measured in an ablation procedure with known geometric parameters (catheter depth and angle).

2. Material and Methods

The ablation model was constructed in SEMCAD, a Finite Element based low frequency solver. A homogeneous slab of tissue 4mm thick was suspended in a blood solution with the catheter incident upon the center of the slab with a dispersive patch electrode on the bottom; this effectively represents a basic ablation scenario. The catheter modeled is a standard 7F, 4mm ablation catheter.

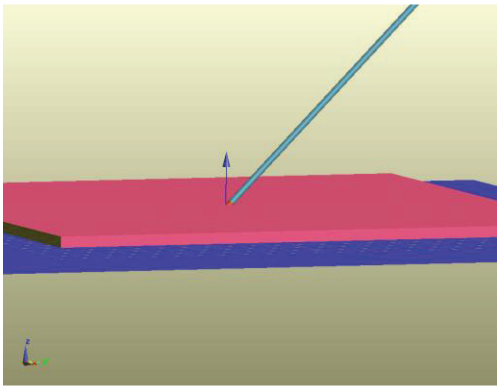

Figure 2. *Sample ablation model setup. Dispersive patch electrode is on bottom in blue, catheter body is in light blue, catheter tip is red and myocardial tissue is pink. Blood fills the rest of the volume. Scenario shown has catheter at 3.2mm depth and 45° angle.*

Since the dimensions of the problem are so small relative to the wavelengths used in typical ablation procedures, the Electroquasistatic assumption was used. This assumption allows the decoupling of the electric and magnetic fields by setting the time varying magnetic field to zero. This assumption allows the transition from a FDTD solution to a frequency domain FEM solution. No flux boundary conditions were used at all edges.

The permittivity and conductivity of both the tissue slab and saline were then carefully chosen using multiple Cole-Cole dispersions [Gabriel et al., 1996] to mimic endocardial tissue and blood. This relationship is described in equation 1.

$$\hat{\epsilon}(\omega) = \epsilon_\infty + \sum_n \frac{\Delta\epsilon_n}{1 + (j\omega\tau_n)^{(1-\alpha_n)}} + \frac{\sigma_i}{j\omega\epsilon_0} \quad (1)$$

where

$\hat{\varepsilon}$ = complex permittivity
ε_∞ = permittivity at high frequency
ε_n = permittivity terms
ε_0 = permittivity of free space
σ_i= Static ionic conductivity
ω= Angular frequency
τ_n= Time constants

Table 1. *Electrical material parameters at 20 kHz used in simulations.*

Tissue Type	*Relative Electrical Permittivity, ε_r*	*Conductivity, σ (S/m)*
Tissue (Myocardium)	37433	0.1717
Blood	5236.5	0.7000

Once an appropriate model is constructed, the impedance can be accurately computed from the electric field values returned by the model. This computation is shown in equation 2.

$$Z = \frac{-\int E \cdot dl}{j\omega \oint_S \tilde{\epsilon}_r E \cdot dS} \qquad where: \tilde{\epsilon}_r = \epsilon_r \epsilon_o - j\left(\frac{\sigma}{\omega}\right) \tag{2}$$

where

E = Electric field
ε_r = Relative permittivity

In a series of simulations, catheter depth and catheter-tissue contact angle were systematically modified and the impedance recomputed. Plots were then generated to correlate catheter/tissue contact area with complex impedance.

Table 2. *Geometric properties of simulations conducted in this study.*

Frequency	*Catheter Depths*	*Angles*
20 kHz	-4 mm	15°
	0.04 mm	30°
	0.8 mm	45°
	1.6 mm	60°
	2.4 mm	75°
	3.2 mm	90°
	4 mm	

3. Results

The first step was to generate plots of impedance parameters at each of the geometric property scenarios described in Table 2. These plots are shown in Figure 3.

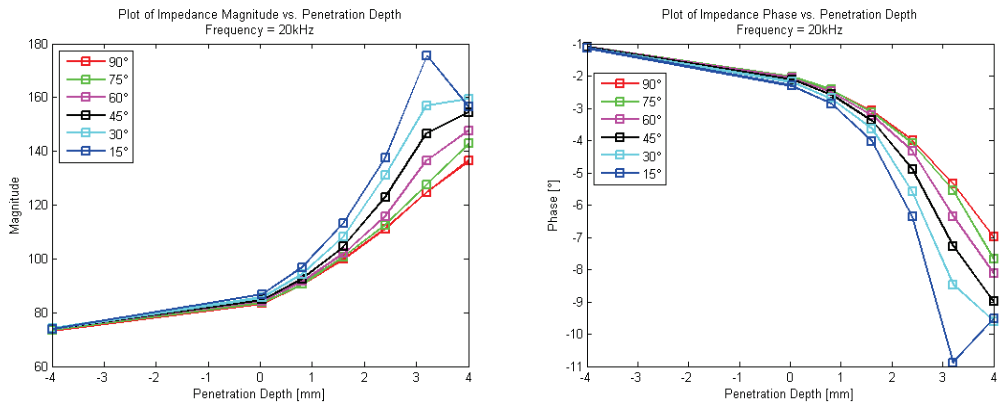

Figure 3. *Plots of the impedance magnitude and phase vs. catheter penetration depth for the different angles.*

We can see that both impedance magnitude and phase tend towards larger values (in absolute) as the catheter gets further engaged into the tissue. Also, magnitude and phase have some angle dependant differences at each penetration depth due to the angle that the catheter is incident upon the tissue. Angle plays a more significant role the deeper the catheter is engaged; when the catheter is in the blood pool (-4 mm) the impedance magnitude and phase are identical for all angles.

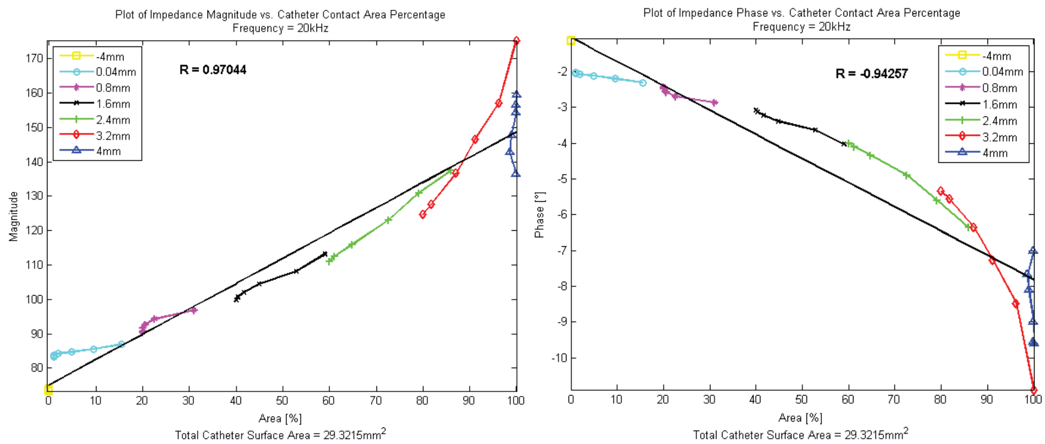

Figure 4. *Plots of Impedance magnitude and Phase vs. catheter/endocardial contact area percentage. Plots are fitted with a linear function and the coerelation coefficient between the impedance parameter and contact area is displayed.*

Figure 4 shows the relation between impedance and catheter/endocardial surface area. Magnitude and phase both have increasing trends with respect to increasing contact area. Points at -4 mm and 4 mm don't follow the established trend.

4. Discussion

Given the comprehensive set of simulations run, it has been shown in Figure 3 that while the impedance magnitude increases markedly with increasing catheter penetration depth, that catheter angle does contribute quite significantly to the measured value. In fact, at a penetration depth of 3.2 mm the calculated impedance is strongly dependant on angle varying from 124.7 at 90° to 175.4 at 15°. The same thing can be observed in the phase plot where at a penetration depth of 3.2 mm the calculated phase varies from -5.348° at 90° to -10.89° at 15°. This can no doubt be explained by the fact that despite having the same penetration depth, angle can have a profound impact on catheter/endocardial surface contact area. In the case considered where the depth is 3.2 mm, the contact area varies from 80% at 90° to 100% at 15°!

In Figure 4 the relationship between the impedance and catheter contact area is more closely explored. Once again, there is an extremely high correlation observed between increasing contact area and both magnitude (R = 0.97044) and phase (R = 0.94257). These plots really illustrate that the impedance depends much more on the contact area than just the depth. The main exceptions to this is when the catheter is in the blood pool (-4mm) and when it is at maximum depth (4mm). When the catheter goes from being in the blood pool to being even slightly engaged with the tissue (1% contact area at a depth of 0.04mm) the impedance seems to spike. Clinically, this is very valuable since it would let the physician know when contact has been made with the tissue. When the catheter is fully engaged (at 4mm depth) the impedance does not continue to increase, as would be dictated by the prevailing trend. This effect is in fact a very interesting one and can most likely be attributed to the fact that the catheter has very nearly penetrated the tissue layer. This observation could be used as a tool to let the physician know that the catheter has very nearly punctured the atrial wall.

The main measured differences in impedance tend to be in magnitude (a max difference of approximately 102.04) and not in phase (max difference of approximately 9.8°). This makes sense as the dominant component of measured impedance is resistance. It cannot however be said that the information that the phase provides is insignificant. At higher frequencies, as with any circuit, the reactive components become smaller. Interestingly though, the rate at which the permittivity and conductivity change with respect to frequency is much different in the blood than in the tissue. This opens the door for some future analysis of complex impedance parameters over a range of frequencies.

5. Conclusions

Establishing and quantifying good catheter/ tissue contact has long been a problem with the RF ablation procedure. Simulation findings in this study indicate that complex impedance can be used as a simple, non-invasive way of solving this problem using existing impedance monitoring capabilities. Consistent relationships exist between impedance and the catheter's geometric contact properties and those relationships can be exploited to provide further information to the physician.

Acknowledgements

This work was supported by the funding of St. Jude Medical and by countless hours from the technical staff at the University of Calgary.

References

Gabriel S., Lau R.W., Gabriel C., The dielectric properties of biological tissues: III. Parametric models for the dielectric spectrum of tissues. *Physics in Medicine and Biology*, 41: 2271-2293, 1996.

Gaita F., Caponi D., Pianelli M., Scaglione M., Toso E., Cesarani F., Boffano C., Gandini G., Valentini M.C., Ponti R.D., Halimi F., Leclercq J.F., Radiofrequency Catheter Ablation of Atrial Fibrillation: A Cause of Silent Thromboembolism? Magnetic Resonance Imaging Assessment of Cerebral Thromboembolism in Patients Undergoing Ablation of Atrial Fibrillation. *Circulation* , 122 : 1667-1673, 2010.

Ho S. Y., Sanchez-Quintana D., Cabrera J. A., Anderson R.H., Anatomy of the Left Atrium: Implications for Radiofrequency Ablation of Atrial Fibrillation. *Journal of Cardiovascular Electrophysiology*, 10: 1525 – 1533, 1999.

Cao H., Tungjitkusolmun S., Choy Y.B., Tsai J.Z., Vorperian V.R., Webster J.G., Using Electrical Impedance to Predict Catheter-Endocardial Contact During RF Cardiac Ablation. *IEEE Transactions of Biomedical Engineering , 49* (3), 247-252, 2002.

Nath S., Lynch C., Whayne J.G., Haines D.E., Cellular Electrophysiological effects of hyperthermia on isolated guinea pig papillary muscle implications for catheter ablation. *Circulation* , 88(1), 1826-1831.

Panescu, D., Whayne J.G., Fleischman S.D., Mirotznik M.S., Swanson D.K, Webster J.G., Three-Dimensional Finite Element Analysis of Current Density and Temperature Distributions During Radio-Frequency Ablation. *IEEE Transactions of Biomedical Engineering* , 879 – 890, 1995.

Wittkampf, F. H.M., Nakagawa H., RF Catheter Ablation: Lessons on Lesions. *PACE* , 29: 1285 – 1297, 2006.